https://doi.org/10.5194/tc-2021-205
Preprint. Discussion started: 22 July 2021

The Cryosphere Discussions
Open Access
EGU

Snow dune growth increases polar heat fluxes

Kelly Kochanski[1,2,3], Gregory Tucker[1,2], and Robert Anderson[1,3]

[1]University of Colorado Boulder, Department of Geological Sciences
[2]University of Colorado Boulder, Cooperative Institute for Research in Environmental Sciences
[3]University of Colorado Boulder, Institute for Arctic and Alpine Research

Correspondence: K. Kochanski (kelly.kochanski@colorado.edu)

Summary

Falling snow often accumulates in dunes. These bedforms are found on up to 14% of the surface of Earth, and appear occasionally on other planets. They have been associated with increased heat fluxes and rapid sea ice melting (Petrich et al., 2012; Popović et al., 2018). Their formation, however, is poorly understood (Filhol and Sturm, 2015; Kochanski et al., 2019a; Sharma et al., 2019). Here, we use field observations to show that dune growth is controlled by snowfall rate and wind speed. We then use numerical experiments to generate simulated dune topographies under varied wind and snowfall conditions, and use those to quantify conductive and radiative heat fluxes through snow. Our results show that dune growth leads to decreased snow cover, more variable snow depth, and significant increases in surface energy fluxes. We provide quantitative results that will allow modelers to account for the impact of snow bedforms in snow, sea ice, and climate simulations. In addition, this work offers a starting point for process-based studies of one of the most widespread bedforms on Earth.

1 Introduction

Snow dunes are ubiquitous on sea ice (Petrich et al., 2012; Popović et al., 2018), common in Antarctica (Doumani, 1967; Mather, 1962; Watanabe, 1978), and seasonally widespread across Siberia, Alaska, Canada, Scandanavia, Japan and the Rocky Mountains (Bagnold, 1941; Colony et al., 1998; Filhol and Sturm, 2015; Sturm and Liston, 2003; Cornish, 1902; Filhol et al., 2017; Kobayashi, 1980; Kochanski et al., 2018, 2019a). Dunes and other bedforms are often encountered by skiiers, snowmobilers, and polar travelers. These areas collectively cover roughly 14% of the surface of the Earth, implying that snow dunes could be one of the most widespread bedforms. They are found, however, in sparsely populated areas, and have received far less scientific attention than dunes of sand.

Existing literature has shown that snow dunes significantly alter the surface energy fluxes. For example, Sturm and Liston (2003) observed that average heat fluxes through Arctic lakes and tundra were twice as high through dune-covered snow as through smooth snow. Several recent studies have shown that dunes control melt on Arctic sea ice by concentrating heat fluxes in narrow inter-dune areas and exposing dark, snow-free ice to the sun (Petrich et al., 2012; Liston et al., 2018; Popović et al.,

https://doi.org/10.5194/tc-2021-205
Preprint. Discussion started: 22 July 2021


The Cryosphere Discussions

2018). Additional literature has shown that other snow bedforms, such as sastrugi, increase surface roughness and turbulent heat transfer (Jackson and Carroll, 1978; Leonard, 2009); snow dunes likely have similar effects.

Finally, there is an extensive literature on the growth of dunes made from sand. Dune growth is an instability that occurs when wind stronger than a critical speed blows over a loose, granular surface (Bagnold, 1941; Werner, 1995; Elbelrhiti et al., 2005). The orientation, shapes, and sizes of the dunes depend on wind direction and sediment supply (Andreotti et al., 2002; Gao et al., 2015), with sediment typically coming from a line or point source upwind of the dune field, such as an eroding rock feature. The dune dynamics may be additionally altered by armoring due to non-uniform grain size (Gao, Xin, Clément Narteau, and Olivier Rozier, 2016) or the erosion of sand particles along the dune field (Jerolmack, D. J., Reitz, M. D., Martin, R. L., 2011). Snow dunes are therefore a special case of dune growth with (1) sediment of lower density and lower average diameter than sand, (2) more fragile and erodible sediment (Comola et al., 2017) than sand, (3) sediment supplied across a wide area from the atmosphere, rather than sediment supplied from a line or point source, and (4) sediment supply that varies over minutes, hours, and days.

In this paper, we focus on the impacts of snow supply and wind speed on dune growth. We show that, unlike sand dunes, which are formed over months or centuries and often reach stable equilibria, snow dunes evolve rapidly during storms and their shapes and sizes change quickly over time.

2 Observations of snow accumulation

We monitored bedform growth for three winters in the Colorado Front Range using time-lapse photography. Four types of surfaces formed in newly deposited snow; they are shown in Fig. 1. Fig. 1a shows *flat snow*, the geometry assumed by most climate and snow science models. Fig. 1b shows thin (< 2 cm) *patches*. These split, merge, and disappear from minute to minute. They typically have narrow upwind ends and one or two downwind points. Fig. 1c shows two *barchan dunes*. These are more stable than patches. They are distinguished by sharp crests and downwind avalanche faces, and move downwind at speeds of up to 2.5 m/h (Kochanski et al., 2019a). Finally, Fig. 1d shows a field of transverse *snow waves*. These have intermittent crests, 3–15 m wavelengths (Filhol and Sturm, 2015), and extend tens or hundreds of meters perpendicular to the wind. Any of these surfaces may be further adorned by small (< 2 cm high) marks, like ripples. Additional imagery and criteria for distinguishing the surface types is given in the supplementary material.

2.1 Statistical methods for field data

The results below summarize observations from three seasons of fieldwork on Niwot Ridge, at 3528 m elevation in the Front Range. The ridge is a natural wind-blown snow laboratory: it receives some dozen large snowstorms each winter, which are blown over the tundra by unidirectional west-northwesterly winds. We were therefore able to observe snow accumulation in the absence of confounding factors like variable wind directions. The winter wind blows consistently west-northwest and averages 10.5 m/s with gusts up to 29.7 m/s. The full observations are archived in Kochanski (2018b); representative excerpts

https://doi.org/10.5194/tc-2021-205
Preprint. Discussion started: 22 July 2021

The Cryosphere Discussions
Open Access
EGU

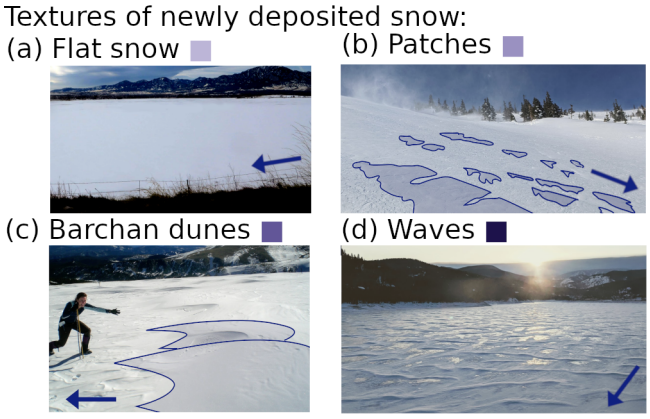

Figure 1. Common textures of newly deposited snow. Arrows mark wind direction. Outlines mark fresh deposits in snow-on-snow photos b and c.

are viewable at Kochanski (2018a). Climate records are drawn from Morse and Losleben (2019). Our data (Kochanski, 2018b) are by an order of magnitude the most extensive snow bedform observations collected to date.

Three experts labeled our time-lapse videos at ten-minute intervals, with labels: 'flat', 'patches', 'dunes', 'waves', 'unidentifiable' and 'not depositional'. Conflicting labels were resolved in favor of the majority. For this study, which focuses on dry, newly deposited snow, we excluded surfaces that had melted (temperature $> -1^{o}$C, the most predictive temperature threshold in our data (Kochanski et al., 2018)) and 'not depositional' observations. The resulting data set was 24% flat snow, 24% patches, 21% dunes, 28% waves, and 3% unidentifiable. These examples, excluding unidentifiable surfaces, are shown as functions of wind speed and time in Figs. 1b and c.

We then built softmax classifiers, a method for separating classes of data by logistic regression, to identify the most likely surface type as a function of weather conditions. We tested classifiers that make predictions using combinations 1–3 of weather variables, from: time, wind speed, gust speed (highest wind speed recorded over each 10 minute interval); and time-averaged wind speed, wind stress, and wind power since snowfall. We excluded wind direction, humidity, and temperature, three variables that had negligible predictive power in previous work with this data (Kochanski et al., 2018).

We quantified the uncertainty in the weather variables using the Monte-Carlo method described in Kochanski et al. (2018), generating 20 data points from each 10 minute video observation, for a total of 11,202 training examples (not an even multiple of 20 because of uncertainty in which observations exceeded melting temperature) representing 93 hours of observations. The classifiers were trained on all labeled examples and were validated by bootstrapping (Efron and Tibshirani, 1985). The uncertainty on the classifiers is the standard deviation of the results of 10 bootstrapping runs plus the one-sigma uncertainty on the parameters from an individual run.

https://doi.org/10.5194/tc-2021-205
Preprint. Discussion started: 22 July 2021

The Cryosphere Discussions
Open Access
EGU

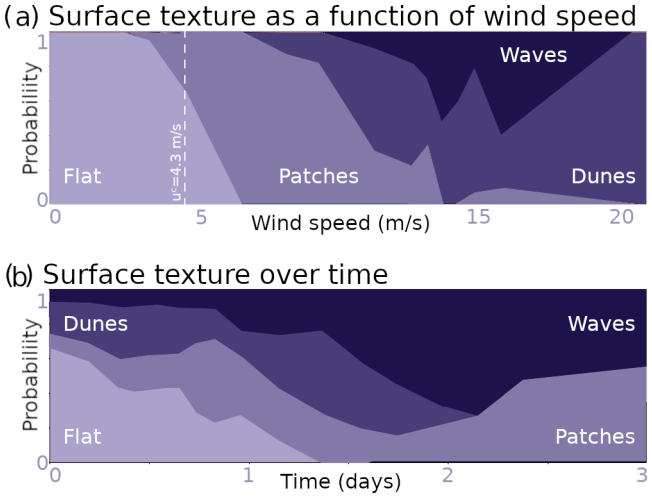

Figure 2. Evolution of snow surfaces in the Colorado Front Range with wind speed and time. (a) Probability of observing surface textures within one day of snowfall as a function of wind speed. (b) Probability of observing surface textures as a function of time.

The presence of flat snow was predicted better by wind speed than by any other variable(s). Dune and wave presence were predicted comparably well by time and wind speed, time and time-averaged wind stress, or time and time-averaged wind power. We use the wind speed classifier in the rest of this text for simplicity and consistency with simulations.

2.2 Fieldwork results

Immediately after snowfall, most snow was flat at wind speeds slower than (4.3 ± 0.9) m/s measured 7.5 m above the surface (Fig. 2a) and most snow was bedform-covered if wind speeds were higher. We hereafter use 4.3 m/s as the value for the critical wind speed, u_c, required to initiate snow saltation and bedform growth at our field site. This value is within the range of previous measurements of u_c for dry snow (Li and Pomeroy, 1997). At wind speeds from 4.3 m/s to 12.0 m/s most snow accumulated in patches, and at wind speeds higher than (12.0 ± 2.7) m/s most snow accumulated in dunes and waves.

Over time, the probability of observing flat and dune-covered snow surfaces decreased while the probability of observing patches and snow-waves increased (Fig. 2b). The flat surfaces were routinely remodeled by strengthening winds; every surface we observed experienced winds higher than 4.3 m/s within 1.5 days of snowfall. Once bedforms grew, the surface did not become flat again unless the bedforms were buried by future storms.

For the next section, we employ a numerical model to explore how snow supply governs transitions between patches, waves, and dunes.

https://doi.org/10.5194/tc-2021-205
Preprint. Discussion started: 22 July 2021


The Cryosphere Discussions
Open Access
EGU

3 Modeling snow morphology as a function of wind speed, snowfall, and time

3.1 Simulation methods

3.1.1 Model set-up

To quantify the 3D dynamics of dune growth in a measurable environment, we simulated accumulation on an initially-flat surface with constant snowfall (s) and constant wind speeds (u). We simulated snow dune growth using Rescal-snow (Kochanski et al., 2019b), an adaptation of sand dune model ReSCAL (Rozier and Narteau, 2014), a community-standard model that has been used in several ground-breaking studies of sand dunes (Gao et al., 2015; Zhang et al., 2012). Rescal-snow is a stochastic 3D cellular automaton that models granular physics through the interactions of neighboring cells, each of which represents a parcel of snow or air. The wind is represented through a lattice gas model. Rescal-snow is fully described by Kochanski et al. (2019b).

We ran fifty simulations. Each modeled 3–7 days of constant snowfall (0.20, 0.63, 2.0, 6.3, or 20 mm/h) blown by constant wind ($u/u_c = 1$, 1.005, 1.05, 1.1, 1.3, 2.0, 2.6, 3.2, 3.9 or 4.5) over an initially flat, bare surface. We modeled a $1200l_0 \times 150l_0$ domain (about $60\mathrm{m} \times 7\mathrm{m}$; unit l_0 is discussed below); this is several times the longest observed bedform wavelength. Snapshots in Fig. 3a, b show a $150l_0 \times 190l_0$ (about $7.5\mathrm{m} \times 9.5\mathrm{m}$) excerpt. Wind was driven and measured along the upper boundary at height 100 l_0 (about 5 m). Grains appeared stochastically along the upper boundary to simulate snowfall, and exited the simulation by blowing through the open downwind boundary. We used periodic wind-parallel boundaries to emulate a wider domain.

3.1.2 Model calibration

We calibrated the length (l_0), time (t_0) and stress (τ_0) scales in the non-dimensional model by matching three simulated quantities to their observable counterparts: the maximum unstable wavelength of a granular bed; the wind speed u/u_c; and the saturated flux of wind-blown snow grains. We assume the following conditions, typical of our field site: snow grains of diameter (0.1 ± 0.05) mm and density (800 ± 100) $\mathrm{kg/m^3}$; air of temperature (-10 ± 2.5)°C (Morse and Losleben, 2019) at 3500 m elevation; surface roughness length $z_0 = (0.24 \pm 0.05)$ mm (Gromke et al., 2011); and threshold wind velocity $u_c = (4.3 \pm 0.9)$ m/s from the field results shown in Fig. 2a. We assume the atmosphere is stable, so that the friction velocity $u_* = u\kappa/\ln(z/z_0)$ for wind velocity u measured at height z and Von Kármán constant $\kappa = 0.4$. We then match several simulated lengths, times, and stresses with their real-world counterparts in order to calibrate the model. The scaling calculations are presented fully in supplementary § S1.3.

The calibration is the dominant source of uncertainty in this simulation. We are able to match lengths and heights to within ±50 %; times to within ±80 %; and wind speeds/stresses to within ±20%. To minimize the impact of this uncertainty, we present most of our results in non-dimensional forms, e.g. snow cover as a fraction of 100% (f); roughness length as a fraction of snow depth (σ/h_{avg}); and heat fluxes through dune-covered snow as a fraction of heat fluxes through uniformly-deep flat

https://doi.org/10.5194/tc-2021-205
Preprint. Discussion started: 22 July 2021


The Cryosphere Discussions
Open Access
EGU

snow (q/q_{flat}). The main exception is the use of results "after 10 cm of snowfall", which to be fully precise should be interpreted as, "after 5–15 cm of snowfall, depending on air density and snow grain size".

3.1.3 Calculating heat fluxes through modeled topography

For the results below, we calculate the average depth of snow, the standard deviation, and the heights of bedforms, in each of our simulations. The average snow depth h_{avg} is the average of the simulated depths; the bedform height is the average distance between maxima and minima on the surface, using filters with a 20 grid cell (≈ 1 m) radius; and the cover fraction f is the fraction of grid cells with non-zero snow depth. All of these quantities are measured over a $100 \times 150 l_0^2$ domain two-thirds of the way toward the downwind end of the domain to avoid edge effects. Calculations were performed in Python using the scipy library (Virtanen et al., 2020).

We also estimate the conductive and radiative heat fluxes through the snow topography for each simulation. We used physical parameters as if the snow fell onto a 35 cm ice floe. We simulated 10 cm of snowfall ($h_{\mathrm{avg}} = 10$ cm), and performed calculations as if it rested on a flat sea ice floe of thickness $h_b = 35$ cm. We used snow and ice albedos $\alpha_s = 0.85 \pm 0.05$ and $\alpha_i = 0.6 \pm 0.1$, and thermal conductivities of $k_s = (0.3 \pm 0.15)$ W/m/K and $k_i = (2.0 \pm 0.2)$ W/m/K. The uncertainties given here represent the natural variability of snow and sea ice for reasons including wetness, snow density and time-dependent metamorphism, ice bubbles, and brine content. To calculate the uncertainties on our final results, we assumed that observed values of α_s, α_i, k_s and k_i were normally distributed, and used a Monte-Carlo simulation to estimate the spread of the resulting heat fluxes. This showed that the variability of the snow and ice albedos and thermal conductivities leads to a 1% variability in the effect of bedforms on conductive heat fluxes, q_C/q_C^{flat}, and a 40% variability in the effect of bedforms on radiative heat fluxes, q_S/q_S^{flat}. This result will be unsurprising to snow scientists, as small changes in snow and ice albedo are known to have huge effects on Arctic thermodynamics.

The conductive heat flux q_C varies with snow thickness, $h(x,y)$, and the thermal conductivities of snow and ice. For simplicity, we calculate the one-dimensional steady-state heat flux:

$$q_C(h_s) \quad = \quad -\int_A \left(\frac{T_s - T_b}{\frac{h_s(x,y)}{k_s} + \frac{h_i}{k_i}} \right) \frac{\partial x \partial y}{A} \tag{1}$$

where A is the sample area and $T_s - T_b$ is the temperature difference between the surface and ice-ocean interface. Fig. 4c presents $q_C/q_C^{\mathrm{flat}} := q_C(h_s)/q_C(h_s = h_{\mathrm{avg}})$. This quantity is independent of temperature. This calculation neglects lateral heat fluxes, and will therefore err on the side of under-estimating the impact of snow dunes on total heat fluxes.

The shortwave radiation flux q_S varies with the snow cover fraction f and the relative albedos of the snow and the surface beneath:

$$q_S(f) \quad = \quad S_0 \left(f(1-\alpha_s) + (1-f)(1-\alpha_b) \right) \tag{2}$$

where S_0 is the incoming shortwave energy flux. Fig. 4d presents $q_S/q_S^{\mathrm{flat}} := q_S(f)/q_S(f=1)$. This quantity is independent of S_0.

https://doi.org/10.5194/tc-2021-205
Preprint. Discussion started: 22 July 2021

The Cryosphere Discussions
Open Access
EGU

3.2 Simulation results

3.2.1 Comparison of observed and modeled snow dunes

Fig. 3a shows how wind speed controls the surface topography after one day of snowfall. Simulated winds at or below the critical speed ($u/u_c \leq 1$) produced flat snow; gentle winds ($1 < u/u_c \leq 2$) produced low-lying patches; moderate winds ($2 < u/u_c \leq 3.2$) mediated a gradual transition from patches to dunes; and high winds ($u/u_c \geq 3.2$) produced well-defined dunes with slip faces. These results agree quantitatively with our field observations, in which flat surfaces only appeared when $u/u_c \leq 1$, and dunes became more common than patches when $u/u_c \geq 2.5 \pm 1.0$. The simulations also demonstrated the mechanism by which dunes and waves co-exist at high wind speeds: when simulated dunes touched arms with their neighbors, they briefly formed long waves, then parted. This process resembles the movement of dislocations in a ripple field, played out at a larger length scale.

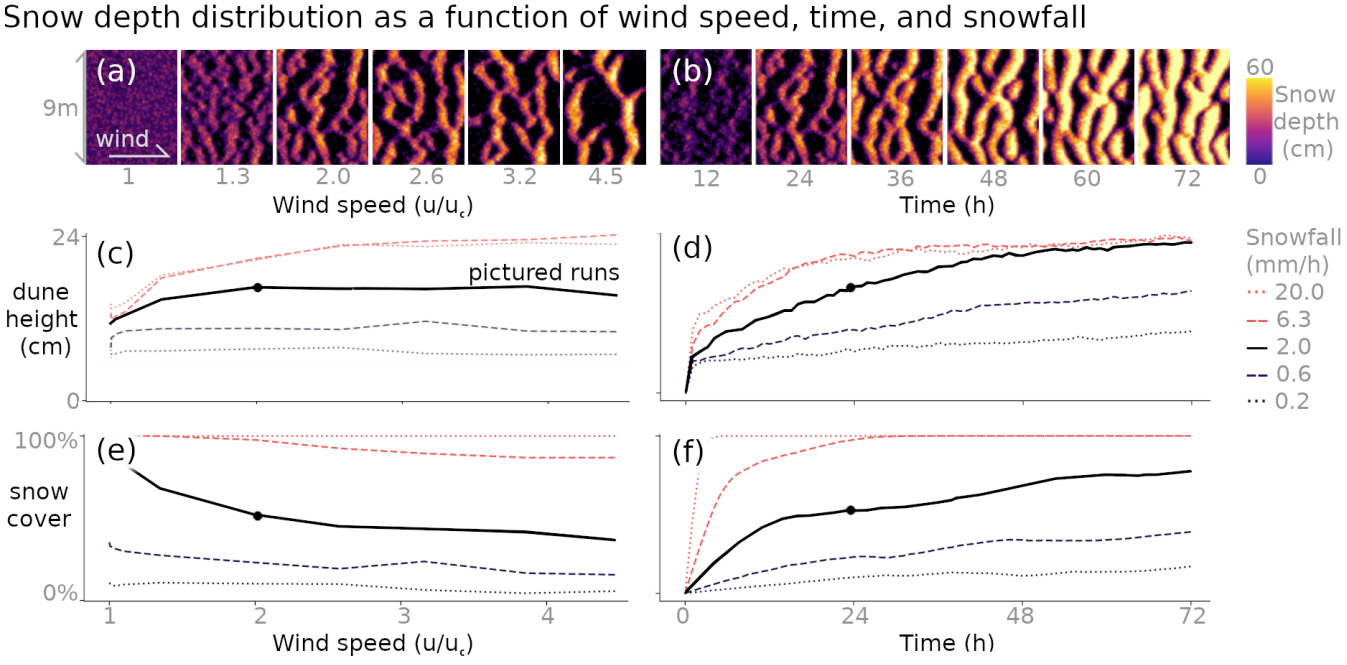

Figure 3. Simulated snow distributions as functions of (a, c, e) wind speed, (b, d, f) time, and snowfall (dashed lines, c–f). Wind speed plots are shown at fixed time 24 h; time plots are shown at fixed wind speed $u/u_c = 2$; black markers show the point common across both. Snowfall rate is fixed at 2 mm/h in a–b.

Fig. 3b shows how dunes grew with time given a constant snow supply (2 mm/h) and a constant wind ($u/u_c = 2$). Snow initially (12 h) collected in patches. After 24–36 h, the patches grew into better-defined dunes, then continued to grow (36–72 h) until they overlapped their neighbors and merged into waves. These results largely agree with our field observations, in which patches were the most likely initial bedform at this wind speed, and dunes transitioned into waves after 24–48 h.

https://doi.org/10.5194/tc-2021-205
Preprint. Discussion started: 22 July 2021

Figs. 3c–f show how bedform growth altered snow depth distribution and cover fraction. Bedforms grew taller with either stronger winds (Fig. 3c) or more time and total snowfall (Fig. 3d). Dunes produced by high winds were widely separated and covered little of the surface (Fig. 3e). In all cases, the surface cover fraction increased with time (Fig. 3f).

Snow that fell faster (Figs. 3c–f, dashed orange lines) formed shorter dunes that covered the surface more quickly than slow-falling snow (dashed purple lines), and thus covering the surface completely with a smaller volume of fallen snow. This occurred because faster snowfall initiated a larger number of dunes than sparse snowfall, with a correspondingly higher surface area to volume ratio.

3.2.2 The impact of dune growth on polar heat fluxes

Bedform size and snow cover fraction both change the surface energy balance, as discussed in § 1. We used our simulated results to quantify the impact of high winds and low snowfall rates on snow depth variability and cover fraction (Figs. 4a–b), over a range of conditions observed on Earth (Fig. 4c). We found that bedforms alter the standard deviation of snow depth by up to 80% in the studied range, and the cover fraction by up to 56%.

We then used simulated snow topographies to estimate changes in conductive and shortwave energy fluxes through 10 cm of snow atop a 35 cm thick ice floe. We normalized these heat fluxes (Fig. 4d–e) by the heat fluxes through flat snow so that the results are thus independent of temperature and radiation intensity (§ 3.1.3).

Fig. 4c shows wind speeds and snowfall rates for seven sites on ice sheets, sea ice, and land, to help readers match the conditions we describe with places they are familiar with. Exact locations, chosen for data availability, are: Savoonga, St. Lawrence Island, Bering Strait; Sapporo, Hokkaido, Japan (Kobayashi, 1972); Niwot Ridge, Colorado, USA (Kochanski et al., 2018); Dumont D'Urville Station, West Antarctica (Grazioli et al., 2017); Summit Station, Greenland; the South Pole (Mahesh et al., 2003); and 70.26°S, 149.99°W in the South Pacific Ocean (Turner et al., 2019). Collectively, these sites represent the full range of global weather, from a desert with extraordinarily low snowfall (the South Pole) to the snowiest region on Earth (Hokkaido, Japan); and from the lowest wind speed (trivially 0 m/s) to a contender for windiest place on Earth (Dumont D'Urville Station, West Antarctica).

Snow dune growth increased the conductive heat flow through the ice by up to 34% within the studied range (Fig. 4d). Dune growth had a greater impact on the balance of shortwave radiation, which it increased by up to 94% (Fig. 4e), as the snow dunes left up to 56% of the less-reflective underlying ice exposed. The magnitude of this radiative effect varies by $\pm 34\%$ with reasonable albedo values for snow and ice. The effect would be much greater if the underlying sub-snow were darker than sea ice (e.g. soil, vegetation, most natural surfaces), and moderately smaller if the surface were brighter (e.g. old snow). If this example ice floe were north of the Arctic circle, and had the largest dunes we simulated (grown from a wind speed of $2u_c$ and snow falling at 0.2 mm/h), dune growth would hasten the conductive winter freezing rate of the floe by 34%, and accelerate the radiation-driven melt rate by 94% in spring.

https://doi.org/10.5194/tc-2021-205
Preprint. Discussion started: 22 July 2021

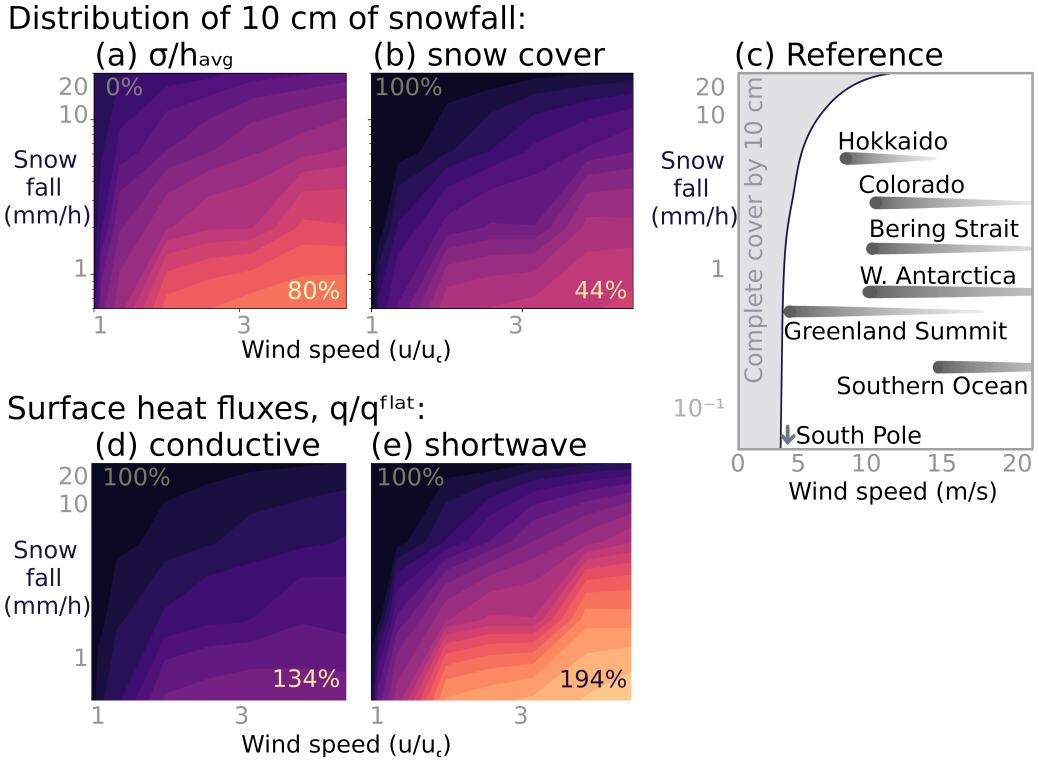

Figure 4. Effects of bedform growth on (a–b) surface morphology and (e–f) surface heat fluxes, as functions of snowfall rate and wind speed u over critical wind speed u_c. Brighter colors indicate stronger bedform effects with contours at 5% intervals. (a) Standard deviation of snow depth σ over average depth $h_{\rm avg} = 10{\rm cm}$ and (b) snow cover fraction. (c) shows average-to-extreme wind speeds and average snowfall rates for selected sites, scaled with $u_c = 4.3$ m/s. (d) Conductive heat flux q through 10 cm of wind-blown snow and 35 cm of ice, over heat flux $q_{\rm flat}$ through flat snow. (e) Same comparison as in (d) but for incoming shortwave energy flux into snow-covered ice.

3.3 Wind-dependent equations for snow cover fraction and surface roughness

Many models of snow cover, sea ice, and the Earth surface include estimates of snow depth, snow cover fraction and surface roughness. The following equations, obtained by statistical fits to our simulation results, allow calculation of those variables accounting for the effects of bedform growth. When the wind speed is small or the snow depth is large, these equations simplify to the forms expected for flat snow.

The snow cover fraction f and standard deviation σ of snow depth obtained from our simulations may be estimated from snowfall rate s (see estimates below), depth of snow fallen $h_{\rm avg}$, and wind speed u/u_c as:

$$f = 1 - \exp\left(-\frac{u}{u_c}\frac{h_{\rm avg}}{h_f}\right) \tag{3}$$

https://doi.org/10.5194/tc-2021-205
Preprint. Discussion started: 22 July 2021

The Cryosphere Discussions
Open Access
EGU

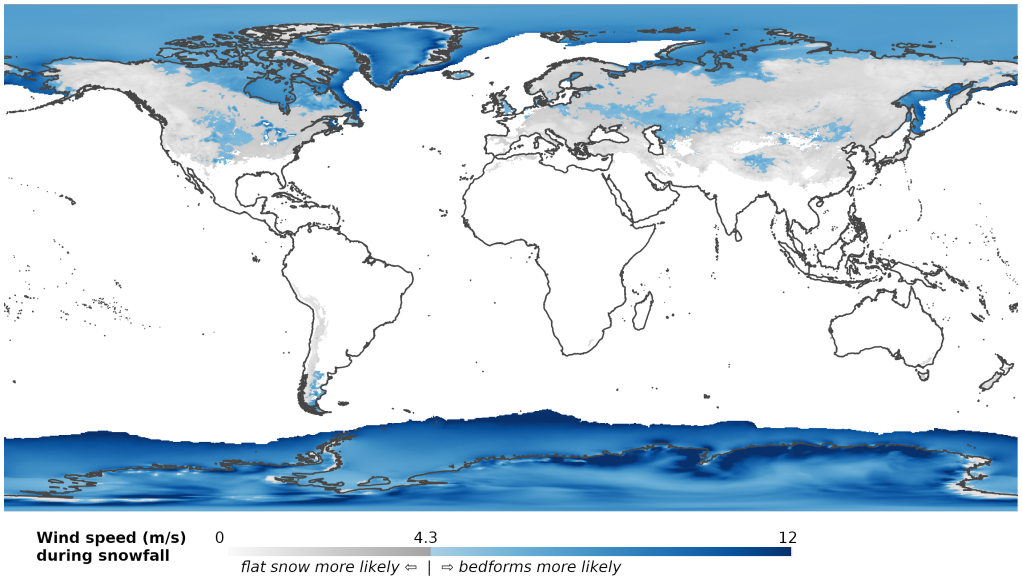

Figure 5. Average 10 m wind speed during snowfall onto sea-ice and snow-covered land, 2010-2020. Dune-forming winds are shown in blue; flat-snow-forming winds are shown in grey. Calculated from monthly reanalysis data (Hersbach, H., Bell, B., Berrisford, P., Biavati, G., Horányi, A., Muñoz Sabater, J., Nicolas, J., Peubey, C., Radu, R., Rozum, I., Schepers, D., Simmons, A., Soci, C., Dee, D., Thépaut, 2018).

$$\frac{\sigma}{h_{\mathrm{avg}}} = \frac{\sigma_{\max}}{h_{\mathrm{avg}}} - \frac{\sigma_0}{h_{\mathrm{avg}}} \exp\left(-\left(\frac{u}{u_c} - 1\right)\frac{h_{\mathrm{avg}}}{h_\sigma}\right) \tag{4}$$

where $h_f = 1700 - 37s$, $\sigma_{\max} = 140$ mm, $\sigma_0 = 110$ mm, $h_\sigma = 54s + 55$, and snowfall rate $0.6 \leq s \leq 20$ mm/h. All lengths are in millimeters; snowfall rates are in mm/h. The fit approximates our simulation results for f to within $\pm 8\%$ and σ to within ± 13 cm.

4 Conclusion

Flat snow should be expected only where winds are consistently slower than the critical speed for snow transport. Such gentle winds are typical of sheltered forests, but not of tundra, ice sheets, sea ice, or the poles (Fig. 5). Snow dunes have been documented in Japan (Kobayashi, 1980), Alaska (Filhol and Sturm, 2015), Colorado (Kochanski et al., 2019a), Antarctica (Doumani, 1967; Gow, 1965), Greenland (Albert and Hawley, 2002), and on Arctic (Petrich et al., 2012) and Antarctic (Massom et al., 2001) sea ice. Dunes may also grow from snowfall on Mars, Titan, and Pluto. Those three bodies likely have solid precipitation (Head et al., 2005; Perron et al., 2006; Telfer et al., 2018) and certainly have dune-forming winds (Hansen et al., 2011; Lorenz et al., 2006; Telfer et al., 2018). For most snow, on Earth and in the solar system, we need not ask whether dunes may form, but instead ask how large they grow, and how much they alter surface thermodynamics.

https://doi.org/10.5194/tc-2021-205
Preprint. Discussion started: 22 July 2021

Code and data availability. Field observations are archived in (Kochanski, 2018b). Dune simulation code is archived in (Kochanski et al., 2019b) and available at http://www.github.com/kellykochanski/rescal-snow.

Author contributions. KK designed the study, performed the fieldwork, wrote and ran the simulation code, analyzed the data, and wrote the manuscript. GT and RSA supervised the project. All authors revised and approved the manuscript.

Competing interests. No competing interests are present

Acknowledgements. We thank E. Hunke, M. Serreze, P. Molnar, and K. Barnhart for useful feedback, and C. Bertholet, C. Herbertson, M. Yoder, R. Barnes and I. Overeem for field assistance. This project was supported by a DOE Computational Science Graduate Fellowship (DE-FG02-97ER25308).

https://doi.org/10.5194/tc-2021-205
Preprint. Discussion started: 22 July 2021

References

Albert, M. R. and Hawley, R. L.: Seasonal changes in snow surface roughness characteristics at Summit, Greenland: implications for snow and firn ventilation, Annals of Glaciology, 35, 510–514, https://doi.org/10.3189/172756402781816591, 2002.

Andreotti, B., Claudin, P., and Douady, S.: Selection of dune shapes and velocities part 1: Dynamics of sand, wind and barchans, European Physical Journal B, 28, 321–339, https://doi.org/10.1140/epjb/e2002-00236-4, 2002.

Bagnold, R. A.: The Physics of Blown Sand and Desert Dunes, Methuen, London, 1941.

Colony, R., Radionov, V., and Tanis, F. J.: Measurements of precipitation and snow pack at Russian North Pole drifting stations, Polar Record, 34, 3–14, https://doi.org/10.1017/S0032247400014923, 1998.

Comola, F., Kok, J. F., Gaume, J., Paterna, E., and Lehning, M.: Fragmentation of wind-blown snow crystals, Geophysical Research Letters, https://doi.org/10.1002/2017GL073039, http://doi.wiley.com/10.1002/2017GL073039, 2017.

Cornish, V.: On snow-waves and snow-drifts in Canada, with notes on the "snow-mushrooms" of the Selkirk Mountains, The Geographical Journal, 85, 342–365, https://doi.org/10.2307/1774538, 1902.

Doumani, G. A.: Surface structures in snow, in: International Conference on Low Temperature Science: Physics of Snow and Ice, pp. 1119–1136, Hokkaido University, Hokkaido, Japan, 1967.

Efron, B. and Tibshirani, R.: The bootstrap method for assessing statistical accuracy, Behaviormetrika, pp. 1–35, 1985.

Elbelrhiti, H., Claudin, P., and Andreotti, B.: Field evidence for surface-wave-induced instability of sand dunes, Nature, 437, 720–723, https://doi.org/10.1038/nature04058, 2005.

Filhol, S. and Sturm, M.: Snow bedforms: A review, new data, and a formation model, Journal of Geophysical Research: Earth Surface, 120, 1645–1669, https://doi.org/10.1002/2015JF003529, 2015.

Filhol, S., Pirk, N., Schuler, T., and Burkhart, J. F.: The evolution of a snow dune field, in: American Geophysical Union, Fall Meeting, pp. C51E–01, New Orleans, LA, USA, 2017.

Gao, X., Narteau, C., Rozier, O., and Du Pont, S. C.: Phase diagrams of dune shape and orientation depending on sand availability, Scientific Reports, 5, 1–12, https://doi.org/10.1038/srep14677, http://dx.doi.org/10.1038/srep14677, 2015.

Gao, Xin, Clément Narteau, and Olivier Rozier: Controls on and effects of armoring and vertical sorting in aeolian dune fields: A numerical simulation study, Geophysical Research Letters, 43, 2614–2622, 2016.

Gow, A. J.: On the accumulation and seasonal stratification of snow at the South Pole, Journal of Glaciology1, 5, 467–477, 1965.

Grazioli, J., Genthon, C., Boudevillain, B., Duran-alarcon, C., Guasta, M. D., Madeleine, J.-b., and Berne, A.: Measurements of precipitation in Dumont d ' Urville, Adélie Land, pp. 1797–1811, 2017.

Gromke, C., Manes, C., Walter, B., Lehning, M., and Guala, M.: Aerodynamic Roughness Length of Fresh Snow, Boundary-Layer Meteorology, 141, 21–34, https://doi.org/10.1007/s10546-011-9623-3, 2011.

Hansen, C. J., Bourke, M., Bridges, N. T., Byrne, S., Colon, C., Diniega, S., Dundas, C., Herkenhoff, K., McEwen, A., Mellon, M., Portyankina, G., and Thomas, N.: Seasonal erosion and restoration of Mars' northern polar dunes, Science, 331, 575–578, https://doi.org/10.1126/science.1197636, 2011.

Head, J. W., Neukum, G., Jaumann, R., Heisinger, H., Hauber, E., Carr, M., Masson, P., Foing, B., Hoffmann, H., Kreslavksy, M., Werner, S., Milkovich, S., van Gasselt, S., and The HRSC Co-Investigator Team: Tropical to mid-latitude snow and ice accumulation, flow and glaciation on Mars, Nature, 434, 2005.

https://doi.org/10.5194/tc-2021-205
Preprint. Discussion started: 22 July 2021

Hersbach, H., Bell, B., Berrisford, P., Biavati, G., Horányi, A., Muñoz Sabater, J., Nicolas, J., Peubey, C., Radu, R., Rozum, I., Schepers, D., Simmons, A., Soci, C., Dee, D., Thépaut, J.-N.: ERA5 hourly data on single levels from 1979 to present, https://doi.org/10.24381/cds.adbb2d47, 2018.

Jackson, B. S. and Carroll, J. J.: Aerodynamic roughness as a function of wind direction over asymmetric surface elements, Boundary-Layer Meteorology, 14, 323–330, 1978.

Jerolmack, D. J., Reitz, M. D., Martin, R. L.: Sorting out abrasion in a gypsum dune field, Journal of Geophysical Research: Earth Surface, 116, 2011.

Kobayashi, D.: Studies of snow transport in low-level drifting snow, Contributions from the Institute of Low Temperature Science, A24, 1–58, 1972.

Kobayashi, S.: Studies on interaction between wind and dry snow surface, Contributions from the Institute of Low Temperature Science, A29, 1–64, 1980.

Kochanski, K.: The movement of snow bedforms in the Colorado Front Range [video] [doi:10.5446/38612], https://doi.org/10.5446/38612, https://av.tib.eu/media/38612, 2018a.

Kochanski, K.: Time-lapse observations of snow bedforms in the Colorado Front Range, 2016-2017 [data set] [doi:10.5281/zenodo.1253725], https://doi.org/10.5281/zenodo.1253725, dx.doi.org/10.5281/zenodo.1253725, 2018b.

Kochanski, K., Tucker, G., and Anderson, R. S.: Statistical classification of self-organized snow surfaces, Geophysical Research Letters, 45, 6532–6541, https://doi.org/10.1029/2018GL077616, 2018.

Kochanski, K., Anderson, R. S., and Tucker, G. E.: The evolution of snow bedforms in the Colorado Front Range and the processes that shape them, Cryosphere, 13, 1267–1281, https://doi.org/10.5194/tc-13-1267-2019, 2019a.

Kochanski, K., Defazio, G.-C., Green, E., Barnes, R., Downie, C., Rubin, A., and Rountree, B.: Rescal-snow: Simulating snow dunes with cellular automata, The Journal of Open Source Software, 4, 1699, https://doi.org/10.21105/joss.01699, 2019b.

Leonard, K. C.: Antarctic Snow Drift Processes, Ph.D. thesis, Columbia University, 2009.

Li, L. and Pomeroy, J. W.: Estimates of threshold wind speeds for snow transport using meteorological data, Journal of Applied Meteorology, 36, 205–213, https://doi.org/10.1175/1520-0450(1997)036<0205:EOTWSF>2.0.CO;2, 1997.

Liston, G. E., Polashenski, C. M., Rosel, A., Itkin, P., King, J., Merkouriadi, I., and Haapala, J.: A Distributed Snow-Evolution Model for Sea-Ice Applications (SnowModel), Journal of Geophysical Research: Oceans, pp. 3786–3810, https://doi.org/10.1002/2017JC013706, 2018.

Lorenz, R. D., Wall, S., Radebaugh, J., Boubin, G., Reffet, E., Janssen, M., Stofan, E., Lopes, R., Kirk, R., Elachi, C., Lunine, J., Mitchell, K., Paganelli, F., Soderblom, L., Wood, C., Wye, L., Zebker, H., Anderson, Y., Ostro, S., Allison, M., Boehmer, R., Callahan, P., Encrenaz, P., Ori, G. G., Francescetti, G., Gim, Y., Hamilton, G., Hensley, S., Johnson, W., Kelleher, K., Muhleman, D., Picardi, G., Posa, F., Roth, L., Seu, R., Shaffer, S., Stiles, B., Vetrella, S., Flamini, E., and West, R.: The sand seas of titan: Cassini RADAR observations of longitudinal dunes, Science, 312, 724–727, https://doi.org/10.1126/science.1123257, 2006.

Mahesh, A., Eager, R., Campbell, J. R., and Spinhirne, J. D.: Observations of blowing snow at the South Pole, Journal of Geophysical Research: Atmospheres, 108, 1–9, https://doi.org/10.1029/2002jd003327, 2003.

Massom, A., Eicken, H., Jeffries, O., Drinkwater, M. R., Worby, P., Lytle, I., Morris, K., Reid, A., and Warren, G.: Snow on Antarctic sea ice, Reviews of Geophysics, 39, 2000RG000 085, 2001.

Mather, K. B.: Further observations on sastrugi, snow dunes and the pattern of surface winds in Antarctica, Polar Record, 11, 158–171, https://doi.org/10.1017/S0032247400052888, 1962.

https://doi.org/10.5194/tc-2021-205
Preprint. Discussion started: 22 July 2021

Morse, J. F. and Losleben, M.: Climate data for saddle data loggers (CR23X and CR1000) 2000-ongoing, daily, Environmental Data Initiative, https://doi.org/10.6073/pasta/cf8ff4f209a889b4b20a4fb48be6f1d8, 2019.

Perron, J. T., Lamb, M. P., Koven, C. D., Fung, I. Y., Yager, E., and Ádámkovics, M.: Valley formation and methane precipitation rates on Titan, Journal of Geophysical Research E: Planets, 111, 1–14, https://doi.org/10.1029/2005JE002602, 2006.

Petrich, C., Eicken, H., Polashenski, C. M., Sturm, M., Harbeck, J. P., Perovich, D. K., and Finnegan, D. C.: Snow dunes: a controlling factor of melt pond distribution on Arctic sea ice, Journal of Geophysical Research: Oceans, 117, https://doi.org/10.1029/2012JC008192, http://doi.wiley.com/10.1029/2012JC008192, 2012.

Popović, P., Cael, B. B., Silber, M., and Abbot, D. S.: Simple Rules Govern the Patterns of Arctic Sea Ice Melt Ponds, Physical Review Letters, 120, https://doi.org/10.1103/PhysRevLett.120.148701, 2018.

Rozier, O. and Narteau, C.: A real-space cellular automaton laboratory, Earth Surface Processes and Landforms, 39, 98–109, https://doi.org/10.1002/esp.3479, 2014.

Sharma, V., Braud, L., and Lehning, M.: Understanding snow bedform formation by adding sintering to a cellular automata model, The Cryosphere, 13, 3239–3260, https://doi.org/10.5194/tc-13-3239-2019, 2019.

Sturm, M. and Liston, G. E.: The snow cover on lakes of the Arctic Coastal Plain of Alaska, U.S.A, Journal of Glaciology, 49, 370–380, https://doi.org/10.3189/172756503781830539, 2003.

Telfer, M. W., Parteli, E. J. R., Radebaugh, J., Beyer, R. A., Bertrand, T., Forget, F., Nimmo, F., Grundy, W. M., Moore, J. M., Stern, S. A., Spencer, J., Lauer, T. R., Earle, A. M., Binzel, R. P., Weaver, H. A., Olkin, C. B., Young, L. A., Ennico, K., Runyon, K., The New Horizons Geology, G., and Team, I. S. T.: Dunes on Pluto, Science, 360, 992–997, https://doi.org/10.1126/science.aao2975, 2018.

Turner, J., Phillips, T., Thamban, M., Rahaman, W., Marshall, G. J., Wille, J. D., Favier, V., Winton, V. H. L., Thomas, E., Wang, Z., van den Broeke, M., Hosking, J. S., and Lachlan-Cope, T.: The Dominant Role of Extreme Precipitation Events in Antarctic Snowfall Variability, Geophysical Research Letters, 46, 3502–3511, https://doi.org/10.1029/2018GL081517, 2019.

Virtanen, P., Gommer, R., Oliphant, T. E., Haberland, M., Reddy, T., Cournapeau, D., Burovski, E., Peterson, P., Weckesser, W., Bright, J., van der Walt, S. J., Brett, M., Wilson, J., Millman, K. J., Mayorov, N., Nelson, A. R. J., Jones, E., Kern, R., Larson, E., Carey, C., Polat, , Feng, Y., Moore, E. W., VanderPlas, J., Laxalde, D., Perktold, J., Cimrman, R., Henriksen, I., Quintero, E., Harris, C. R., Archibald, A. M., Ribeiro, A. H., Pedregosa, F., van Mulbregt, P., and SciPy 1.0 Contributors: SciPy 1.0: Fundamental Algorithms for Scientific Computing in Python, Nature Methods, pp. 1–12, 2020.

Watanabe, O.: Distribution of Surface Features of Snow Cover in Mizuho Plateau, Memoirs of National Institute of Polar Research. Special issue, 7, 44–62, 1978.

Werner, B. T.: Eolian dunes: computer simulations and attractor interpretations, Geology, 23, 1107–1110, https://doi.org/10.1130/0091-7613(1995)023<1107:edcsaa>2.3.co;2, 1995.

Zhang, D., Narteau, C., Rozier, O., and Courrech Du Pont, S.: Morphology and dynamics of star dunes from numerical modelling, Nature Geoscience, 5, 463–467, https://doi.org/10.1038/ngeo1503, http://dx.doi.org/10.1038/ngeo1503, 2012.